



Preferential CO oxidation in hydrogen (PROX) on ceria supported catalysts

PART II. Oxidation states and surface species on Pd/CeO₂ under reaction conditions, suggested reaction mechanism

O. Pozdnyakova¹, D. Teschner^{1,2*}, A. Wootsch¹, J. Kröhnert², B. Steinhauer², H. Sauer²,
L. Toth³, F. C. Jentoft², A. Knop-Gericke², Z. Paál¹, R. Schlögl²

¹Institute of Isotopes, CRC, HAS, POB 77, Budapest, H-1525, Hungary

²Department of Inorganic Chemistry, Fritz-Haber-Institute of the MPG, Faradayweg 4-6, 14195 Berlin, Germany

³Research Institute for Technical Physics and Materials Science, HAS, Budapest, POB 49, H-1525, Hungary

* Corresponding author: e-mail teschner@fhi-berlin.mpg.de, phone +49 30 8413 5408, fax +49 30 8413 4676

Abstract

The aim of the PROX reaction is to reduce the CO content of hydrogen feed to proton exchange membrane fuel cells (PEMFC) by selective oxidation of CO in the presence of excess hydrogen. Both Pt and Pd on ceria are active in CO oxidation (without hydrogen) while Pd is poorly active in the presence of hydrogen. In this paper we aimed at finding the reasons of such behavior, using the same techniques for Pd/CeO₂ as for Pt/CeO₂ in Part I: catalytic tests, in-situ DRIFTS, high-pressure XPS, HRTEM and TDS. The reaction mechanism of CO oxidation (without hydrogen) was also examined. It does not occur via the exactly same mechanism on Pt and Pd/CeO₂ catalyst. In the presence of hydrogen (PROX) at low temperature (T=350-380 K), the formation of Pd β-hydride was confirmed by high-pressure in-situ XPS. Its formation greatly suppressed the possibility of CO oxidation, because oxygen both from gas phase and support sites reacted fast with hydride H to form water, and this water desorbed from Pd easily. Nevertheless, CO adsorption was not hampered here. These entities transformed mainly to surface formate and formyl (-CHO) species instead of oxidation as observed by DRIFTS. The participation of a low-temperature water-gas-shift type reaction proposed for the platinum system [Part I] was hindered. Increasing temperature led to decomposition of the hydride phase and a parallel increase in the selectivity towards CO oxidation was observed. However, it remained still lower on Pd/CeO₂ than on Pt/CeO₂.

Keywords: Hydrogen purification; fuel cell; preferential CO oxidation; PROX; palladium; palladium-hydride; Pd/CeO₂; ceria; high pressure XPS; in situ DRIFT; TDS; HRTEM

1. Introduction

The importance of the PROX reaction has been described in detail in the Introduction of the first part of this paper [1]. Briefly, for the proper operation of proton exchange membrane fuel cell (PEMFC), the CO content of the hydrogen feed must be kept, as a rule, under 1-100 ppm [2]. The aim of the *preferential oxidation* reaction (PROX) is to oxidize selectively CO reducing its concentration from 1-1.5 % to under 100 ppm without oxidation of the excess hydrogen present [1,3,4].

Catalyst formulations found to be active in the PROX reaction can be classified as: gold based catalysts

[5-8], supported Pt [5,8-12], Rh [9], Ru [9,13], and bimetallic Pt-Sn [11,14] and other systems not containing metallic phase, such as CuO/CeO₂ [5,15]. These systems, as a rule, are also active in the low temperature CO oxidation. Palladium based catalysts represent a class of its own: while Pd on different supports, especially on those active in the transient oxygen storage (such as ceria) is remarkably active in CO oxidation [16-20], it shows very low selectivity towards CO oxidation in the presence of hydrogen [9,21-23].

This low activity/selectivity of Pd in the PROX reaction has not been elucidated yet in detail. A group of authors [9,12] explains this fact by the change in the oxidation state of Pd. The highly active reduced Pd form

(active in low temperature CO oxidation) can be oxidized to PdO_x, which is less active in CO oxidation (without hydrogen). This change occurred around 360 K on Pd/Al₂O₃ in the presence of oxygen [9]. The authors stated that this PdO_x is very active in hydrogen oxidation, while it shows low activity in CO oxidation, thus low selectivity in the PROX reaction. It was also suggested that other metals, like Au or Pt, cannot be oxidized as easily as Pd, and the rate of CO oxidation on their metallic form is higher than that of H₂ oxidation. Nevertheless, this tentative proposition was not supported by any experimental evidence.

In this paper, we studied the PROX reaction on Pd/CeO₂ catalysts, active in CO oxidation both in the presence [19] and absence of oxygen (OSC) [24,25], using the same experimental methods as in the first part [1], namely catalysis, high-pressure XPS, TDS, HRTEM, and in situ DRIFT spectroscopy. The aim of this paper is to clarify the reaction mechanism of both CO oxidation and the PROX reaction on a Pd catalyst, study the role of the reducible ceria support, and to compare its behaviour with Pt/CeO₂, which was found to be remarkably active in the PROX reaction [1,12].

2. Experimental

2.1. Catalysts

Two catalysts with nominally 1% and 5% metal loadings were prepared on the same ceria support used in Part I [1] (Rhodia Catalysts & Electronics, France, BET=96 m² g⁻¹, [26]) by wet impregnation with aqueous solution of Pd(NH₃)₄(NO₃)₂ [12,27]. The impregnated samples were dried at 393 K overnight and calcined for 4 hours at 773 K in flowing air (30 mL/min) and reduced at 672 K for 4 hours in flowing H₂ (30 mL/min). Dispersion was determined by low temperature (223 K) H₂ adsorption after reduction [28,29]. The received values were D=68% for 1% Pd/CeO₂ and 23% for 5% Pd/CeO₂.

2.2. Catalysis

Catalytic tests were carried out in the same atmospheric continuous flow reactor system as in the first part [1], using stainless steel tubing, connections and analytical grade gases controlled by mass-flow controllers. Products were analysed by (i) a gas-chromatograph (TCD) equipped with a polar column, Poropak Q separating CO₂ and H₂O from the other outlet gases, and (ii) by a hydrogen compensated flue-gas analyzer (type: MRU DELTA 65-3) for CO and O₂ quantification. Methane formation did not occur on Pd catalysts; CO₂ and H₂O were detected as only products, similar to Pt [1]. The total gas inlet was 100 NmL/min, containing 1% CO, 0.4-1% O₂ (oxygen excess, λ, from 0.8 to 2) and the rest was H₂.

The catalysts were activated in situ in flowing air (30 mL/min) at 573 K, before catalytic tests. A charge of 95 mg 1% Pd/CeO₂ and 83 mg 5% Pd/CeO₂ was used in the catalytic reactor and reactivated between different measurement series by the above mentioned treatment [12]. CO and O₂ conversion, as well as the selectivity were calculated as previously [1,12].

2.3. Temperature programmed desorption (TDS)

Different gas mixtures were adsorbed at room temperature on the 5% Pd/CeO₂: (i) CO+O₂ (10⁻² mbar O₂ + 2*10⁻² mbar CO for 20 min), and H₂+CO+O₂ (4.7*10⁻¹ mbar H₂ + 2*10⁻² mbar CO + 10⁻² mbar O₂ for 20 min). After adsorption the sample was evacuated and transferred to the UHV part of the setup to follow the desorption pattern (heating rate 1 K/s). For more details see Part I.

2.4. In situ diffuse reflectance infrared spectroscopy (DRIFTS)

DRIFTS experiments were carried out under the same conditions as in Part I [1], with the same Bruker spectrometer. Inlet gases were analytical grade and were controlled by mass-flow controllers. The total gas flow was 50 NmL/min, containing 1% CO in N₂ (referred to as *CO alone*), 1% CO, 1% O₂ in N₂ (*CO+O₂*) or 1% CO, 1% O₂ in H₂ (*PROX*).

All measurements were carried out on a ca. 100 mg fresh sample previously pre-treated in situ in flowing air (30 mL/min) at 573 K. The catalyst was purged in N₂ while cooling down to the desired reaction temperature of 383 or 523 K, respectively. A spectrum of the activated sample before adsorption was collected in N₂ at the reaction temperature and then the reaction mixture – pre-mixed in a bypass – was introduced to the catalyst in one step. Spectra were collected as a function of time on stream for 90 minutes in all cases. Only spectra under steady state conditions will be shown.

The gas composition was analyzed only in the case of the PROX reaction by a mass spectrometer. Selectivity and activity values were calculated using the same formula as presented earlier [1].

2.5. High pressure X-ray Photoelectron Spectroscopy (XPS)

The in-situ XPS experiments were performed at beam line U49/2-PGM2 at BESSY in Berlin. Ce 3d, O 1s, Pd 3d, and C 1s spectra were recorded with photon energies of hv = 1035, 920, 725 and 670 eV. The binding energies were calibrated using internal references, such as the Ce 3d V (882.4 eV) and U''' (916.7 eV) hybridization states or the Ce 4f state in the band gap. Decomposition of the Pd

3d, O 1s and C 1s regions were performed using Gauss-Lorentz curves, except the metallic Pd 3d component at 335 eV, which was fitted using a Gauss-Lorentz profile with exponential tail. The 5% Pd/CeO₂ pellet (~ 100 mg) was activated in-situ in oxygen (0.5 mbar, 573 K). The PROX mixture contained 0.45 mbar H₂, 0.031 mbar CO and 0.015 mbar O₂. Gas phase analysis was carried out using a quadrupole Balzers mass spectrometer. For more details, see Part I.

2.6. High Resolution Transmission Electron Microscopy (TEM)

HRTEM investigations were performed in a Philips CM200 FEG electron microscope operated at 200 keV. The microscope was equipped with a Gatan imaging filter (GIF 100), Gatan Slow-Scan-Camera and an EDX system. The sample was prepared from a piece of 5% Pd/CeO₂ that was previously activated in O₂ and used in the PROX mixture in the in-situ XPS cell (as was done for the in-situ XPS experiments).

3. Results

3.1. Catalytic reaction

Figure 1 shows the CO oxidation activity on the 1% Pd/CeO₂ catalyst in the absence of hydrogen. The sharp “light off” observed on Pt/CeO₂ [1] was also found here when excess oxygen was used (Figure 1), while it was less pronounced on Pd when $\lambda \leq 1$ was applied than on Pt under the same conditions.

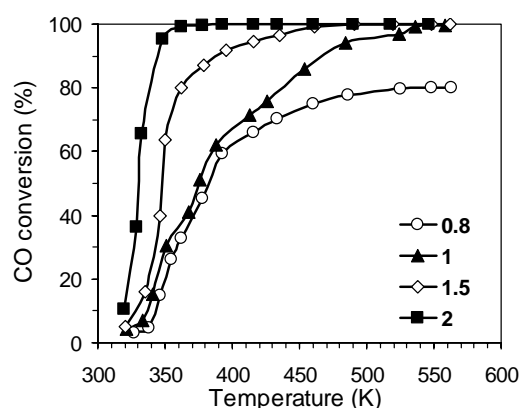


Figure 1: Conversion of carbon monoxide on 1% Pd/CeO₂ at different oxygen excess, λ (in the absence of hydrogen).

In the presence of hydrogen (Figure 2), the oxygen conversion was very high on Pd/CeO₂ (Figure 2) – around 98-100% – similar to that on Pt/CeO₂ [1,12]. On the other hand, the CO conversion was very low on Pd/CeO₂ and increased as a function of temperature as opposed to

Pt/CeO₂ [1,12]. This increase was rather steep up to 380 K, and then only little variation was observed. Interestingly, the CO conversion was almost independent of the oxygen excess used (Figure 2a). Figure 2d presents hydrogen conversion values calculated as the consumption of the inlet excess hydrogen. Their nominally low values are due to the high hydrogen excess present in the inlet stream. Hydrogen oxidation was enhanced by the higher excess of oxygen i.e. by higher $p(O_2)$. As the CO conversion was more or less independent of λ , the CO₂ selectivity pattern (Figure 2c) is dictated by the enhanced hydrogen conversion at higher oxygen excess. The actual selectivity values (Figure 2c) were much lower on Pd than on Pt, in good agreement with earlier data [9,21-23].

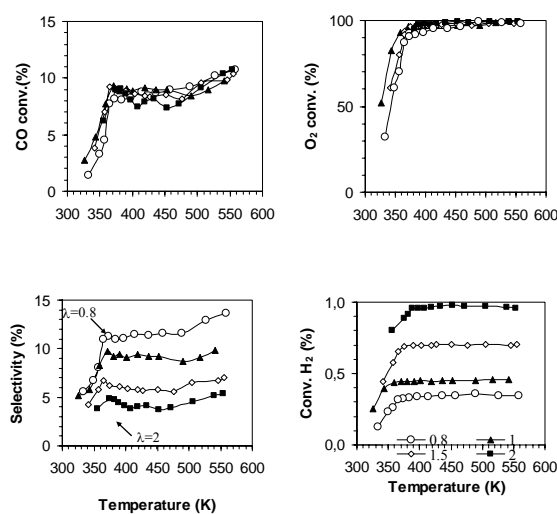


Figure 2: The PROX reaction on 1% Pd/CeO₂ catalyst at different oxygen excess, λ . CO oxidation activity in the presence of hydrogen (a), oxygen conversion (b), selectivity towards CO oxidation (c) and conversion of the excess hydrogen (d).

Similar to the methodology used in Part I, the 5% Pd/CeO₂ catalyst was measured in the high-pressure XPS apparatus and the 1% sample in DRIFTS experiments, while both of them were tested in the catalytic reactor. The different results are compared in Table 1. The activity pattern showed similar trends with different actual values (Table 1). In the catalytic reactor, the almost total oxygen conversion was accompanied by ca. 10% CO conversion independent of the reaction conditions. In the spectroscopic apparatus, the lower contact time (and much higher dead-volumes than in the catalytic reactor [1]) manifested itself in lower oxygen conversion values.

Summarizing the catalytic results, Pd/CeO₂ catalysts showed much lower selectivity towards CO oxidation in the presence of hydrogen than Pt/CeO₂, especially at low temperature (365-385 K), at about the same high oxygen conversion, using approximately the same mass of catalyst with about the same dispersion. On the other hand, this formulation was active in CO oxidation without hydrogen (Figure 1).

3.2. Temperature programmed desorption (TDS)

Figure 3 shows the desorption curves of CO₂ for 5% Pd/CeO₂ after adsorbing different gas mixtures at ambient temperature. For comparison the corresponding data of the platinum catalyst are also included. Both catalysts reveal very similar CO₂ desorption curves when no hydrogen was added, with a broad first maximum at ~ 400 K and a second maximum at or above 573 K. The first is attributed to CO₂ formed on metallic particles, while the second is due to CO₂ desorbing from the support. In the presence of hydrogen, however (i) the first broad peak separates into two peaks: a narrow one at lower (~ 360 K) and a second one at higher temperature (~ 440-450 K); (ii) the amount of CO₂ desorbing in the narrow peak is roughly three times less for Pd/CeO₂ than for Pt/CeO₂ and (iii) the desorption pattern above 450 K is the same for the two samples. Water formation was similar for both catalysts (slightly lower for Pd), while a significant amount of hydrogen desorbed from Pd/CeO₂ (not shown).

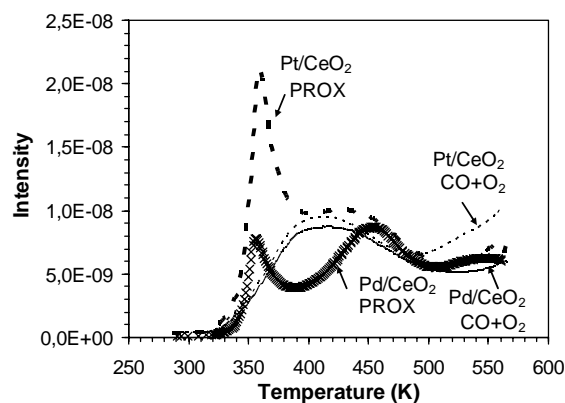


Figure 3: Temperature programmed desorption (TDS) curves of CO₂ from the 5% loading catalysts after adsorbing different gas mixtures at room temperature: CO+O₂ to 10⁻² mbar O₂ + 2*10⁻² mbar CO for 20 min, and PROX mixture 4.7*10⁻¹ mbar H₂ + 2*10⁻² mbar CO + 10⁻² mbar O₂ for 20 min. Pt/CeO₂ in CO+O₂: thin dashed line. Pt/CeO₂ in PROX: thick dashed line. Pd/CeO₂ in CO+O₂: thin full line. Pd/CeO₂ in PROX: xxx.

3.3. In-situ DRIFTS

DRIFT spectra in the region 2200-1800 cm⁻¹

The DRIFTS spectra of 1% Pd/CeO₂ at 383 and 523 K under CO alone, CO+O₂ and PROX conditions in the region 2200-1800 cm⁻¹ are shown in Figure 4. Bands observed were denoted following the original assignments of Palazov et al. [30]. Adsorption of CO alone (Figure 4a) produced strong bands at 2082 cm⁻¹ (L₂) (with significant broadening at the low-frequency side) and ca. 1971 cm⁻¹ (B₂) as well as weak bands at 2177, 2152 and 2135 cm⁻¹ (L₃). The broad tail towards lower wavenumbers of the strong L₂ band contains a component at ca. 2065 cm (L₁).

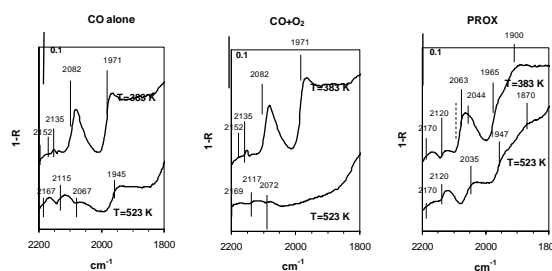


Figure 4: DRIFT spectra in the 2200-1800 cm⁻¹ region - CO vibrations - of 1% Pd/CeO₂ in the presence of a) 1% CO alone in N₂ b) in 1% CO and 1% O₂ in N₂ and c) in 1% CO and 1% O₂ in H₂ - PROX at 383 and 523 K, respectively.

The ν(CO) bands above 2000 cm⁻¹ are attributed to terminal, mono-coordinated or linearly bonded carbon monoxide, while the broad, convoluted bands under 2000 cm⁻¹ are assigned to multi-coordinated CO [31]. The L₂ and L₃ bands were ascribed to the linear adsorption of CO on Pd⁰ and Pd^{II} sites, respectively [30]. The asymmetrical broad B₂ band is attributed to the bridged adsorption of CO on Pd⁰ sites. The doublet encompassing weak broad bands at 2177 and 2152 cm⁻¹ was ascribed to CO linearly adsorbed on oxidized ceria sites [32], overlapping with the gas-phase CO.

Increasing temperature leads to (i) almost complete disappearance of the L₂ and L₁ bands, (ii) appearance of a broad feature at 2115 cm⁻¹, and (iii) shift of the B₂ band to lower wave numbers (from ca. 1971 to ca. 1945 cm⁻¹). The broad feature at ~2115 cm⁻¹ might encompass contributions from CO stretching on Ce³⁺ as well as on Pd^{II} sites.

The presence of oxygen (Figure 4b) in the gas mixture did not affect the position and intensities of the ν(CO) bands at T=383 K, while at elevated temperature no bands of multi-coordinated CO and a general decrease in the band intensities were observed.

Under PROX conditions at T=383 K, (i) the broad L₁ band with an additional feature at ca. 2044 cm⁻¹ dominates the spectra, while L₂ becomes obscured by the intensive L₁ band; (ii) the intensity of B₂ decreases significantly while a very broad band formed at ca. 1900 cm⁻¹ (B₁). Increasing temperature in the presence of hydrogen leads to (i) a general decrease in intensities and a shift of the bands to lower wavenumbers: main band from 2063 to ca. 2035 cm⁻¹, B₁ band from 1900 to ~1870 cm⁻¹ and B₂ band from 1965 to 1947 cm⁻¹; (ii) decrease in the relative intensity of the broad feature observed at ca. 2170 cm⁻¹ (ν(CO) on Ce⁴⁺ sites) and increase of that at ca. 2120 cm⁻¹. The range of positions of the B and L bands observed might be due to changes in the CO coverage upon different experimental conditions [31,33,34]. Downshift and decrease in the intensities of B bands at higher temperature and in the presence of H₂ as well as decrease in the relative intensity of the L₂ band and increase of the L₁ band in the presence of H₂ at T=383 K indicate lower CO coverage at higher temperature and in H₂-rich atmosphere.

DRIFT spectra in the region 1800-1000 cm⁻¹

Similarly to the Pt/CeO₂ catalyst [1], a large variety of carbonate species (OCO vibrations) are present on the O₂ pre-treated sample (Figure 5). Mainly uni- and/or polydentate carbonate (giving strong bands at 1465 and 1359 cm⁻¹ and a weak band at 1080 cm⁻¹) and traces of bidentate carbonate (bands at 1566, 1300 and 1019 cm⁻¹), bicarbonate (medium bands at 1390, 1227 and weak bands at ca. 1609 and 1050 cm⁻¹) and carboxylate (1516 cm⁻¹) species are present on the surface of the O₂ pre-treated sample at T=383 K. Increasing temperature (Figure 5b) resulted in a decrease of the bicarbonate and bidentate carbonate species on the surface of the activated sample.

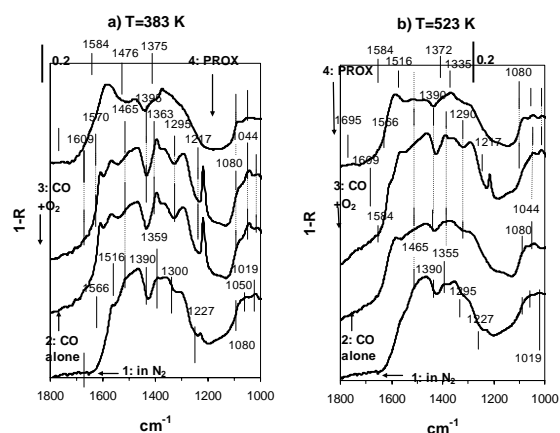


Figure 5: DRIFT spectra in the 1800-1000 cm⁻¹ region - OCO vibrations - of 1% Pd/CeO₂ at **a)** T=383 K and **b)** T=523 K after activation, in the presence of 1% CO alone in N₂, in 1% CO and 1% O₂ in N₂, and in 1% CO and 1% O₂ in H₂ - PROX, respectively.

Exposure to CO alone or in the presence of oxygen at T=383 K (Figure 5a) yields bands characteristic of (i) bicarbonate species: strong bands at 1609, 1395 and 1217 cm⁻¹ and a medium band at 1044 cm⁻¹; and (ii) bidentate carbonate species: $\nu(\text{CO}_3)$ bands (at 1570 and 1295 cm⁻¹). Under PROX conditions, bicarbonate species, which were observed in the H₂-free gas mixture, do not form, while $\nu(\text{CO}_3)$ bands of uni- and bidentate carbonate species of the same intensities are present in the spectra. At the same time, the spectrum became dominated by a strong broad band centered at ca. 1584 cm⁻¹ and medium one at 1375 cm⁻¹. These bands were assigned to $\nu_{\text{as}}(\text{OCO})$ and $\delta(\text{CH})$ vibrations of bridged formate species on the ceria surface. Accordingly, a strong $\nu(\text{CH})$ band at 2838 cm⁻¹ appeared (Figure 7). The $\nu_{\text{s}}(\text{OCO})$ band of bridged formate species was poorly resolved at ca. 1330 cm⁻¹.

At T=523 K, the presence of CO alone over Pd/CeO₂ did not affect significantly the positions and intensities of the bands corresponding to different carbonate species present on the surface (Figure 5b). An additional feature at ca. 1584 cm⁻¹ appeared, which is assigned to $\nu_{\text{as}}(\text{OCO})$ vibration of bridged formate species, further supported by the appearance of strong $\nu(\text{CH})$ band at 2847 cm⁻¹ (Figure 7). Exposure to the CO+O₂ gas mixture at T=523 K resulted in

spectra very similar to that observed at T=383 K, except that the bands of bicarbonate species were of significantly lower intensities. Under PROX conditions at elevated temperature a slight decrease in the intensities of the $\nu_{\text{as}}(\text{OCO})$ and $\delta(\text{CH})$ bands of formate species at 1584 and 1372 cm⁻¹, respectively, was observed as compared to in PROX conditions at T=383 K. The small feature at 1335 cm⁻¹ with the weak band at 1516 cm⁻¹ and the small contribution (1695 cm⁻¹) on the broad shoulder at ca. 1600 cm⁻¹ reflect the presence of carboxylate and hydrated carboxylate species on the surface.

DRIFT spectra in the region 3800-3100 cm⁻¹

After oxidative pre-treatment of the 1% Pd/CeO₂ sample, mainly three OH groups at 3708 (with weak band at 3684), 3653 (with shoulder at 3625 cm⁻¹) and 3516 cm⁻¹ (with shoulder at 3427 cm⁻¹) were resolved as shown in Figure 6. The sharp band at 3708 cm⁻¹ was assigned to mono-coordinated OH (I) groups, the broad band at 3653 cm⁻¹ and the shoulder at ca. 3625 cm⁻¹ have been assigned to two types of doubly bridging OH (II-A and II-B, respectively) groups, while a broad band centered at 3516 cm⁻¹ was assigned to triply bridging OH (III) species [35]. Increase of the temperature resulted in a slight (~10 cm⁻¹) down-shift of all $\nu(\text{OH})$ bands and a decrease in the number of mono-coordinated (OH-I) hydroxyl groups on the ceria surface.

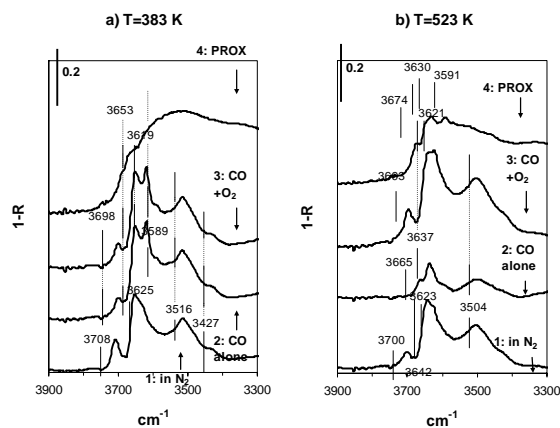


Figure 6: DRIFT spectra in the 3900-3300 cm⁻¹ region - OH vibrations - of 1% Pd/CeO₂ at **a)** T=383 K and **b)** T=523 K after activation, in the presence of 1% CO alone in N₂, in 1% CO and 1% O₂ in N₂, and in 1% CO and 1% O₂ in H₂ - PROX, respectively.

Exposure to CO at T=383 K over Pd/CeO₂ results in (i) immediate appearance of a strong $\nu(\text{OH})$ band at 3619 cm⁻¹ and a weak broad band at ca. 3589 cm⁻¹; (ii) significant decrease in intensity and shift to lower (3698 cm⁻¹) wavenumbers of the $\nu(\text{OH-I})$ band. The development of a strong band at 3619 cm⁻¹ and the decay of the band at 3708 cm⁻¹ were attributed to the formation of HCO₃⁻ species (accordingly to the corresponding $\nu(\text{CO}_3)$ bands in Figure 5) through reaction of CO with terminal (OH-I) hydroxyl

groups. The presence of oxygen had no effect on the positions and relative intensities of the $\nu(\text{OH})$ bands of isolated OH groups. Upon CO adsorption at elevated temperature $\nu(\text{OH})$ bands were down-shifted, as compared to at $T=383$ K, with significant decrease in the intensities of the $\nu(\text{OH-I})$ and $\nu(\text{OH-II})$ bands (Figure 6b). In the presence of oxygen more intense bands were observed.

Upon introduction of the PROX gas mixture at $T=383$ K, isolated peaks convolute into intense and broad absorption features becoming difficult to follow individually, similar to Pt/CeO₂ [1]. We attributed this feature to adsorbed water (with hydrogen bonding to surface OH groups and to each other) on the ceria surface in the case of Pt/CeO₂. Its overall intensity on Pd/CeO₂ was lower than on Pt/CeO₂. At $T=523$ K, however, three well-resolved bands of isolated OH groups were observed at 3674 (denoted as OH-IIA*), 3630 (OH-IIB) and 3591 cm⁻¹. Shoulders and less well-defined adsorption features were also observed, among which those centered at ca 3648 (OH-IIB*), 3520, 3450 and 3320 cm⁻¹ were the most visible. The difference between the $\nu(\text{OH})$ (II-B) and (II-B*) wavenumbers (3630 and 3648 cm⁻¹) may be due to different cerium oxidation states [35] involving surface or subsurface reorganization [35,36]. The $\nu(\text{OH})$ band at 3591 cm⁻¹ indicates the presence of hydrated carboxylate species (-COOH) on the surface of ceria support.

DRIFT spectra in the region 3000-2600 cm⁻¹

After oxidative treatment of the Pd/CeO₂ sample no bands were observed in the region 3000-2600 cm⁻¹, while exposure to CO alone or in the presence of oxygen at $T=383$ K gave weak broad absorption features at ca. 2880-2840 cm⁻¹ (Figure 7). Under *steady-state* PROX conditions a strong band at 2838 cm⁻¹ (with a well-resolved shoulder at 2812 cm⁻¹) and weaker broad bands at 2947, 2907, 2736 and 2713 cm⁻¹ were observed. The main bands were assigned to formate species on the ceria surface [37,38,39] as follows: 2838 cm⁻¹ as $\nu(\text{CH})$, 2947 cm⁻¹ as combination of $\nu_{\text{as}}(\text{OCO})$ at ~ 1580 cm⁻¹ (Figure 5) and the C-H in-plane vibration, 2736 cm⁻¹ as overtone $2\delta(\text{C-H})$ ($\delta(\text{C-H}) \sim 1375$ cm⁻¹ in Figure 5). The pronounced shoulder at 2812 cm⁻¹ and the broad band centered at 2713 cm⁻¹ could be due to C-H stretching vibrations of formyl species [38].

Increasing temperature (Figure 7b) under conditions of CO alone resulted in a $\nu(\text{CH})$ band at 2847 cm⁻¹ and a combination mode band at 2947 cm⁻¹. In the presence of oxygen at elevated temperature no distinct bands were resolved in this region. Under PROX conditions at $T=523$ K (i) the position of the maximum of the $\nu(\text{CH})$ band shifted to 2832 cm⁻¹ (with a poorly resolved shoulder at ca. 2848 cm⁻¹); (ii) the band of the formyl species at 2812 cm⁻¹ is not resolved anymore, and that at 2713 cm⁻¹ decreases and shifts to 2711 cm⁻¹.

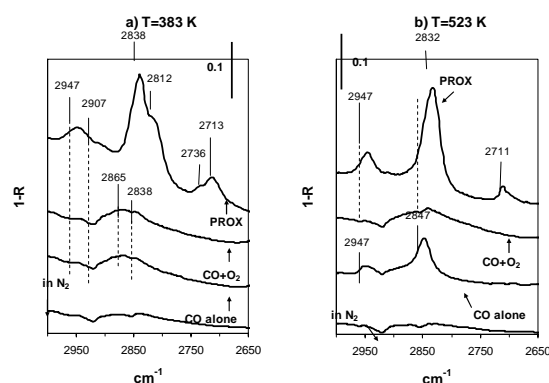


Figure 7: DRIFT spectra in the 3000-2650 cm⁻¹ region - CH vibrations - of 1% Pd/CeO₂ at **a)** $T=383$ K and **b)** $T=523$ K after activation, in the presence of 1% CO alone in N₂, in 1% CO and 1% O₂ in N₂, and in 1% CO and 1% O₂ in H₂ - PROX, respectively.

3.4. High pressure XPS

The same procedure was carried out with the palladium sample as described for Pt/CeO₂ [1]: activation in 0.5 mbar O₂ at 573 K, cooling down in O₂, and at ~ 340 K oxygen was exchanged to hydrogen (0.45 mbar). At room temperature, first CO (0.031 mbar) and then O₂ (0.015 mbar) were added to the hydrogen. The reaction was run with this mixture at 358 and 523 K. The surface state of the sample was investigated in these different environments. The catalytic activity observed during high-pressure XPS measurements is presented in Table 1.

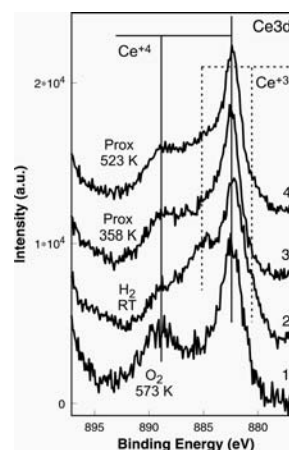
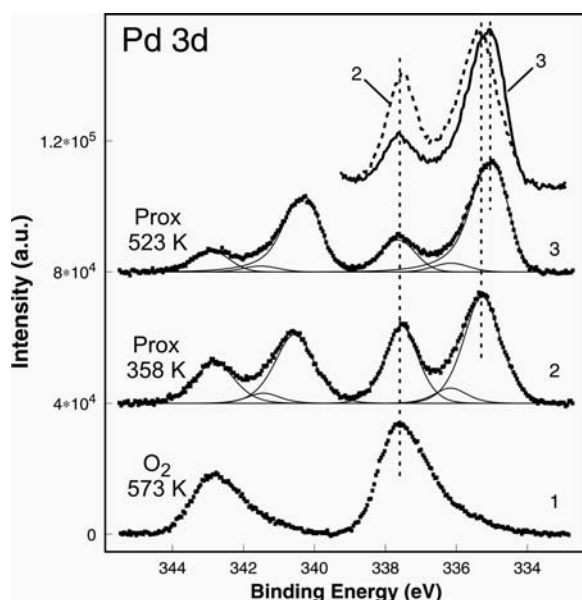


Figure 8: Part of the Ce 3d region of the 5% Pd/CeO₂ at different conditions: **1**, in 0.5 mbar O₂ at 573 K; **2**, in 0.48 mbar H₂ at RT; **3**, in ~ 0.5 mbar PROX mixture at 358 K; **4**, in ~ 0.5 mbar PROX mixture at 523 K; the measurements were carried out in sequence as indicated by the numbers.

Figure 8 depicts part of the Ce3d region in oxygen (573 K), in hydrogen (300 K) and in the PROX mixture. The cerium 3d signal of Pd/ceria behaved in these different conditions very similar as in case of Pt/ceria, thus the surface state of ceria is not affected by the different nature of

Table 1: PROX reaction in different experimental setups and on different catalysts. Reaction mixtures contained 1% CO, 0.5 or 1% O₂ (O₂ excess $\lambda=1$ or 2) in H₂. Total pressure: P=1 atm in catalytic reactor and DRIFT cell and P=0.5 mbar in high pressure XPS.

Conditions	Catalytic reactor						DRIFTS		XPS			
	Catalyst	1% Pd/CeO ₂		5% Pd/CeO ₂		1%Pd/CeO ₂		5%Pd/CeO ₂				
O ₂ excess (λ)	1	1	2	2	1	1	2	2	2	2	1	1
T (K)	383	523	383	523	383	523	383	523	383	523	358	523
X _{CO} , %	9	9	9	10	10	11	9	12	4	10	1	8
S, %	9	9	5	5	10	11	5	6	3	6	6	17
X _{O₂} , %	96	99	98	100	97	100	99	100	70	82	14	53


Figure 9: Pd 3d region of 5% Pd/CeO₂ at different conditions: **1**, in 0.5 mbar O₂ at 573 K; **2**, in ~ 0.5 mbar PROX mixture at 358 K; **3**, in ~ 0.5 mbar PROX mixture at 523 K

precious metal particles. Ce was in the +4 state in oxygen. Hydrogen induced the reduction of the topmost layer to Ce³⁺. In the PROX mixture Ce was almost completely re-oxidized. The only difference was that at 358 K in the PROX mixture cerium in Pd/CeO_x was slightly more oxidized and no further oxidation occurred at 523 K.

Activation of the sample in O₂ at 573 K brought the palladium particles in an almost completely oxidized PdO₂ state seen by the 2.6 eV BE shift (with respect to the metallic state) in Figure 9. Tailing in the low-BE side might be caused by some partly reduced states; however an asymmetric broadening of the PdO₂ peak by differential charging cannot be excluded. Charging of ~ 8 eV was observed in O₂, while in the PROX mixture it was as low as 2 eV. Hydrogen introduced at 340 K reduced a part of the palladium. Metallic-like Pd (~ 335.3 eV) was predominant over

PdO₂ during reaction at 358 K. At higher reaction temperature the contribution of PdO₂ decreased, while the low-BE component shifted -0.25 eV to 335.05 eV, i.e. to the position of bulk metallic palladium. Closer inspection of the low-BE component revealed that its shape was roughly symmetric at 358 K, and the well-known asymmetry of Pd3d evolved just at higher T (see the upper part of Figure 9). The different form and binding energy position of the low-BE component can be well explained by the formation of a hydride-like structure in the excess of hydrogen at low T, which decomposes at elevated temperature [40]. Formation of β -hydride is effectively enhanced by (i) the limited size of nanoparticles [41], (ii) the presence of adsorbed CO that promotes H bulk dissolution, as it reduces the H diffusion barrier between surface and subsurface sites by about 50% [42], (iii) and by the hindrance of oxygen diffusion from the PdO₂ core still remaining below the metallic shell of Pd particles. Non-destructive depth profiling on the Pd 3d core level (by using different excitation energies, thus different photoelectron kinetic energies) indicated that PdO₂ was at least partly below the low-BE component, i.e. below the hydride. As surface hydride decomposed, the further reduction of PdO₂ was more effective. Curve fitting of the PROX spectra provided an intermediate binding energy component at ~ 336.1 eV. Considering the surface core level shift of 0.94-0.99 eV when CO is linearly adsorbed on palladium single crystals [43-45], the small 336.1 eV peak can be attributed to surface palladium atoms adsorbing CO. Thus, the Pd 3d spectra do not indicate the presence of a high amount of adsorbed CO on palladium.

The carbon 1s spectrum of Pd/ceria in the PROX mixture at 358 K (not shown) reveals a similar picture as the platinum sample at 523 K, with a high amount of graphite/C-H and a low amount of adsorbed CO. The only difference was that the component at about 288.2 eV (most probably surface formates) was more pronounced for Pd/CeO_x.

In the first part of our paper we concluded that surface water species are formed during the reaction, which

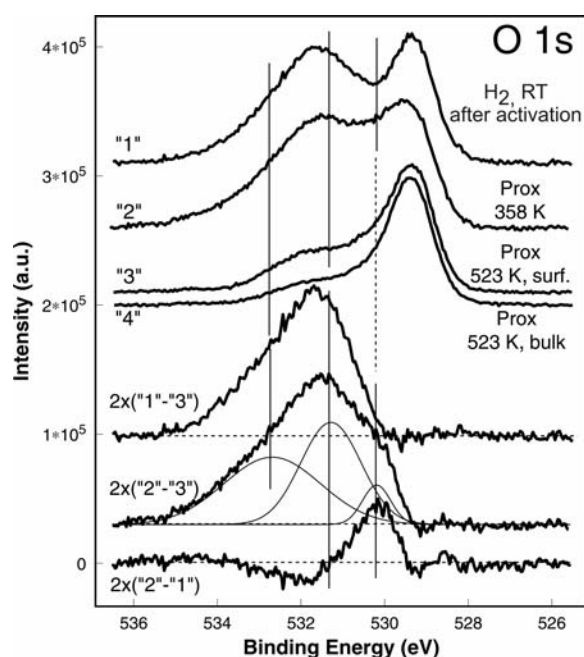


Figure 10: O 1s spectra of 5% Pt/CeO₂ at different conditions: **1**, in 0.48 mbar H₂ at RT (after O₂ activation at 573 K); **2**, in ~ 0.5 mbar PROX mixture at 358 K; **3&4**, in ~ 0.5 mbar PROX mixture at 523 K; **3**: measured with surface sensitive (650 eV) photon energy (as **1&2**, as well) while **4** was measured with more bulk sensitive energy (920 eV). Some difference spectra are also shown.

can play a crucial role in the oxidation mechanism. Therefore we discuss the O 1s spectra of both catalysts in this part together. In the upper part of Figure 10 selected O 1s spectra of Pt/ceria are depicted at different conditions, while the lower part shows some difference spectra. Spectra 1-3 were taken with surface sensitive photon energies whereas spectrum 4, the same reaction condition as 3, was measured with a more bulk sensitive photon energy. The comparison of spectrum 3 and 4 confirms that the high-binding-energy part of the O 1s spectrum belongs to surface species. Therefore the peak at 529.4 eV corresponds to oxygen in the ceria lattice (bulk oxygen), in agreement with earlier studies [46,47]. The O-to-Pt atomic ratio was roughly in the range of 100, thus all the information in the high BE side of O 1s should necessarily correspond to the surface of ceria. (Changes in the scale of 0.2-1 % in the oxygen spectra are not distinguishable.) In hydrogen a strongly pronounced broad peak overlapped with the lattice oxygen component, indicating the presence of OH groups on the surface. This peak was asymmetrically broadened to the high energy side, as seen in the upper difference curve, involving already surface water. (As shown by the DRIFTS data, different carbonates exist on the surface of ceria already in the activated state, which should contribute to this part of the O 1s signal.) Introduction of CO + O₂ to the hydrogen (and heating to 358 K) resulted in a small loss of intensity in the OH region and a new component at ~ 530.2 eV appeared. This feature corresponds to some newly formed oxygenate from CO on the support. Interestingly,

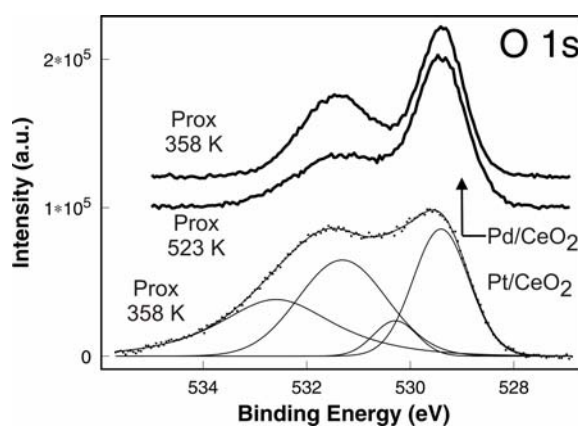


Figure 11: Comparison of O1s spectra of 5% Pt/CeO₂ and 5% Pd/CeO₂ in PROX mixture.

the reoxidation of ceria (see Ce 3d) was not accompanied by a significant loss of OH groups, therefore the presence of OH groups does not necessarily indicate that cerium is in the +3 oxidation state. Heating to 523 K removed gradually most of the high BE components. Figure 11 shows the O 1s spectra of Pd/ceria during the reaction together with the low T spectrum of the platinum sample. The relative intensity of the surface components is considerably lower on Pd/ceria, and especially the components at 530.2 and 532.7 eV are missing. The latter peak corresponded to water. Its lower amount points to the importance of surface water in the reaction mechanism, as Pd/ceria is ineffective to remove CO in a hydrogen excess. The difference between the O 1s spectra of the two samples was much smaller at higher temperature (compare Figure 10 and 11).

3.5. High-resolution TEM

High-resolution TEM measurements were carried out on the post-reaction 5% Pd/CeO_x sample (used in the XPS cell at 0.5 mbar PROX mixture at 358 K). Part of the ceria particles were still in the oxidized CeO₂ state (mainly with some lattice distortion), but part of them were reduced. However, crystalline Ce₂O₃ has never been observed. Figure 12 depicts a typical reduced ceria particle with its power spectrum. After Fast-Fourier-Transformation of the selected part of the image, the power spectrum indicated inverse lattice fringes not permitted in CeO₂. Comparison with possible partly reduced ceria phases revealed the presence of CeO_{1.695}, in which the ordering of oxygen vacancies leads to the formation of a super-cell structure with a lattice constant slightly more than twice that of CeO₂ [48]. Some of the reflections are indexed in the power spectrum for the CeO_{1.695} phase. The fraction of reduced ceria was less in Pd/CeO_x compared to the platinum sample after the same reaction treatment.

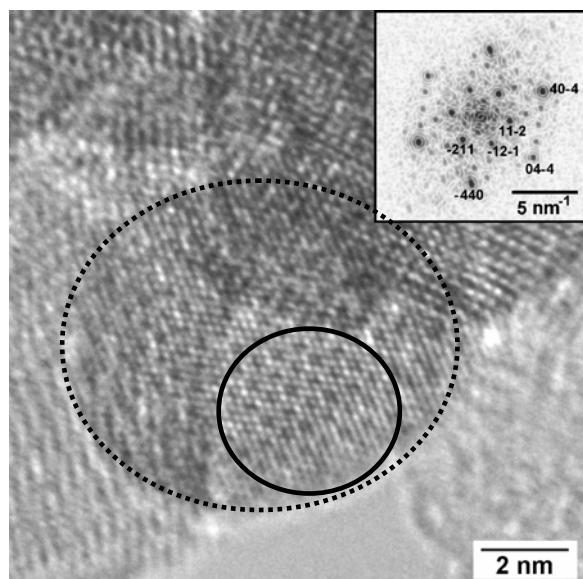


Figure 12: High-resolution TEM image of 5% Pd/CeO₂ after PROX reaction at 358 K. The inset shows the power spectrum of the selected area (full circle) revealing a partly reduced ceria particle (CeO_{1.695}). The dotted line indicates the dimension of the reduced ceria particle.

4. Discussion

Both ceria supported Pt and Pd catalysts are active in low temperature CO oxidation [16-20], cf. results on Pt/CeO₂ in the Part I [1] and on Pd/CeO₂ in Figure 1. However, Pd/CeO₂ exhibits a much lower activity in CO oxidation reaction, when it was carried out in the presence of excess hydrogen (PROX) [9,21-23], cf. catalytic results presented on Pt/CeO₂ in Part I [1] and on Pd/CeO₂ in Figure 2. In this paper we aimed at explaining these large differences, considering surface species, oxidation states and reaction mechanism.

The first principal question is whether CO oxidation (without hydrogen) occurs via the same mechanism on Pt and Pd/ceria catalysts. It was concluded [1] that the CO coverage is rather high on Pt particles, and oxygen from support sites promotes CO₂ formation, both in CO alone and CO+O₂ case. In the latter case, gas phase oxygen can re-oxidize the ceria surface.

In the case of pre-oxidized Pd/CeO₂ fewer CO molecules are adsorbed on the metal particles, estimated from the DRIFTS results (Figure 4) and from transmission IR data not presented in this study, than in the case of Pt/CeO₂ pretreated similarly [1]. Particularly at T=523 K, M-CO bands on Pd/ceria were poorly developed, and almost completely disappeared in CO+O₂ (Figure 4). At the same time, high pressure XPS showed an oxidized, PdO₂ state during the oxidizing pretreatment (Figure 9). PdO_x is reportedly less active in CO oxidation than reduced metallic Pd [9]. Nevertheless, we found remarkable activity of pre-oxidized Pd/CeO₂ in CO oxidation (Figure 1). Consequently, CO oxidation on pre-oxidized ceria supported Pd and Pt does

not occur exactly the same way due to the different affinity of Pt and Pd to oxygen. Palladium particles are oxidized, and thus adsorb less CO than Pt particles. This adsorbed CO can react with oxygen from PdO_x particles, which can then be replenished by oxygen either from the gas-phase or from the support.

It was also concluded in the case of Pt/CeO₂ that not only back spill-over of oxygen from the support to the metal particles is possible, but also spillover of CO (or CO₂) to the support (and/or direct adsorption of CO on the support). These processes lead to accumulation of different carbonate species on ceria, mainly bicarbonate (HCO₃⁻) species upon exposure to CO or CO+O₂ at low temperature. At higher temperature this species is decomposed and CO₂ is also produced this way (as observed by TDS as well). Accordingly, a similar reaction pathway can be suggested for Pd/ceria as well. The pronounced formation of bicarbonate species was observed at low temperature here, too (Figure 5 and 6).

Let us remember the original question of this work: “why Pd is not active and selective in the PROX reaction (CO oxidation in the presence of H₂) although both Pt and Pd on ceria are active in CO oxidation (without hydrogen)”? It was proposed earlier [9] that the highly active reduced Pd form (active in low temperature CO oxidation) is oxidized to PdO_x around 360 K, which is, in fact, less active in CO oxidation but very active in hydrogen oxidation. It was also suggested that other metals, like Au or Pt, cannot be oxidized as easily as Pd, and the rate of CO oxidation on their metallic form is higher than that of H₂ oxidation. This tentative proposition, however, was not supported by any experimental evidence.

In order to clarify this issue, the differences observed in the PROX reaction between Pt/ceria (part I [1]) and Pd/ceria (this paper) in various experiments are summarized:

- (i.) Pd/CeO₂ exhibits much lower selectivity towards CO₂ formation in the PROX reaction than Pt/CeO₂.
- (ii.) The selectivity (S) towards CO oxidation first sharply increased as a function of temperature from 330 K to 360 K, then a slight increase was observed on Pd/CeO₂; on the other hand, S (from much higher value) decreased continuously as a function of T on Pt/CeO₂.
- (iii.) More hydrogen and less water desorbed from Pd than from Pt in the TDS experiment. Roughly three times more CO₂ desorbed from Pt/ceria in the first sharp TDS peak (at temperature optimal for Pt/CeO₂ in PROX reaction).
- (iv.) Less CO is adsorbed on Pd than on Pt indicated by IR results.
- (v.) At T=383 K, much more formate species were found on Pd than on Pt and their amount slightly decreased on Pd, while greatly increased on Pt as temperature in-

creased. Also, there is a negative correlation between the intensity of the C-H stretching band of formates and the amount of CO₂ produced (part I, [1]). Additionally, formyl species were found on Pd at low temperature as opposed to Pt, but they were not observed at higher temperature.

- (vi.) More adsorbed water was found on the ceria surface of Pt/CeO₂ than on Pd/CeO₂, observed by both, high pressure XPS in the O1s spectra (Figure10) and in the DRIFT spectra.
- (vii.) Ceria was slightly more oxidized (less reduced) at low T under PROX condition in the case of Pd/ceria than in Pt/ceria (XPS). However, this slight difference disappeared at higher temperature.
- (viii.) Formation of Pd β -hydride could be detected on Pd/ceria, as opposed to no hydride formation on Pt.

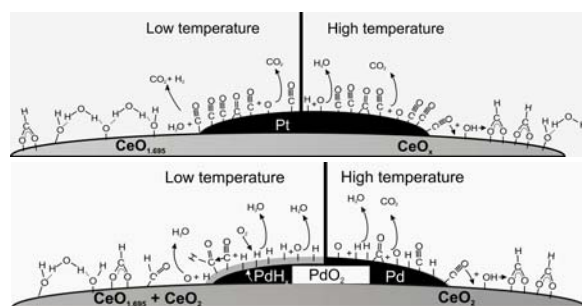


Figure 13: Proposed models describing the reactions happening on **a**, Pt/ceria and **b**, Pd/ceria in the PROX reaction mixture at low and high temperature.

On the bases of the above mentioned differences, different reaction pathways can be proposed for ceria supported Pd and Pt catalysts in the PROX reaction. Their simplified visualization is presented in Figure 13. On the platinum sample at low temperature, a low-temperature water-gas-shift type reaction was suggested at the Pt/ceria interface between the linearly adsorbed CO molecules (on Pt) and the adsorbed water (on ceria). As reported recently [49], such reaction may occur directly (COads+ H₂Oads or OH groups) or via carboxylate intermediates, which are present in our case [1]. The by-product hydrogen before desorption (or another hydrogen molecule from the gas-phase) regenerates the water structure on the support in the close vicinity of Pt. This adsorbed water, which ensures that CO is linearly bonded to the interface Pt site, might be stabilized by the oxygen-deficient character of ceria (CeO_{1.695}). At higher temperature the hydrogen-bonded structure decomposes and water desorbs allowing the liberation of coordinatively unsaturated (cus) Ceⁿ⁺ sites at the interface. Thus CO can adsorb at the interface in a bridged-like manner, oxygen coordinating to this cus site. The adsorbed CO can then dissociate or hop to the ceria and react with an OH group forming formates. The latter species are

stable on the ceria at this condition and might block the way of still existing surface water to the Pt particles. The negative correlation of surface formates and CO₂ yield strengthens the proposed model.

At low temperature (T=358-385 K) in the PROX mixture H dissolves in Pd particles forming a hydride-like structure (Figure 9). At the same time, CO adsorption is not hindered (Figure 4), but CO oxidation may occur at a low rate, since the selectivity is very low. The reason might be that such a structure dramatically decreases the possibility of the reaction between CO adsorbed on metal particles and oxygen either from the gas phase or from the support, because oxygen reacts very fast with H on the hydride surface during the formation of water. This water most probably desorbs or might move to the support, stabilized in hydrogen-bonded structure similar to Pt/CeO₂ [1]. Such a structure, indeed, was observed on Pd/ceria by DRIFTS (Figure 6), but in much lower amount than on Pt/ceria, as also confirmed by XPS (Figure 11). Consequently, water preferentially desorbs from Pd under reaction condition. The much higher affinity of palladium to hydrogen might be one reason why the hydrogen spillover to the support is less pronounced, thus (i) the surface of ceria is slightly less reduced, (ii) fewer CeO_{1.695} particles were found and (iii) less water is formed and stabilized on the ceria surface as compared to the Pt/CeO₂ case. Less water on the ceria surface, less linearly adsorbed CO on Pd and more formates probably on the way between water and CO might be an additional important factor why Pd/ceria is much less active in CO oxidation in the presence of hydrogen.

Increasing the temperature leads to decomposition of the Pd β -hydride to metallic Pd as found by XPS (Figure 10). Parallel to the decomposition of hydride-like structure, the selectivity towards CO oxidation sharply increased as a function of temperature up to ~380 K and then remained almost constant with a slight increase (Figure 2). The presence of small adsorbate-induced Pd in XPS (Figure 9), and poorly discernable M-CO bands in DRIFT (Figure 4) indicate a low CO coverage on the metallic Pd phase at T=523 K. Consequently, metallic Pd might still adsorb hydrogen rather than CO. Further, the remaining PdO₂ surface is supposed to oxidize hydrogen faster than CO [9]. These two facts might be the reason why the selectivity towards CO oxidation is still lower on Pd/CeO₂ than on Pt/CeO₂ at high temperature, even though no Pd-hydride phase was present here.

5. Conclusions, Summary

The aim of this paper was to examine the PROX reaction on ceria supported Pd catalyst by different, mainly in situ experimental techniques, and to answer the question why both Pt and Pd catalysts are active in CO oxidation and Pd is not active in the presence of hydrogen.

It is concluded that CO oxidation (without hydrogen) does not occur via the same mechanism on Pt and Pd/CeO₂ catalysts. On pre-oxidized Pd/CeO₂, CO is adsorbed at low

coverage and reacts with oxygen from the PdOx phase. This oxygen can then be substituted either from the gas phase or from the support. On the other hand, the CO coverage on Pt/CeO₂ is high and adsorbed CO reacts with oxygen from the support. On both samples, spillover of CO to the support and/or its direct adsorption and accumulation as carbonate species and finally their desorption in the form of CO₂ is a possible reaction route in the absence of hydrogen.

In the presence of hydrogen (PROX) at low temperatures T=350-380 K, formation of Pd β-hydride was evidenced from high-pressure in-situ XPS. Its formation greatly suppressed the possibility of CO oxidation, because oxygen both from gas phase and support sites (and also from PdO_x) reacts fast with H to form water, and this water desorbs easily. Nevertheless, CO adsorption was not hampered here. These entities turned partly to surface formate and formyl (-CHO) species instead of oxidation. The involvement of LTWGS type reaction was also hindered by the (i) smaller amount of water on the ceria surface, (ii) less linearly adsorbed CO on Pd and (iii) significantly more formates species blocking the reaction, compared to Pt/CeO₂.

References

- [1] Part I.
- [2] A. J. Appleby, F. R. Foulkes, Fuel Cell Handbook, Van Nostrand Reinhold, New York, 1989.
- [3] C. D. Dudfield, R. Chen, P. L. Adock, Int. J. Hydrogen Energy 26 (2001) 763.
- [4] S. H. Lee, J. Han, K-Y Lee, J. Power Sources 109 (2002) 394.
- [5] G. Avgouropoulos, T. Ioannides, Ch. Papadopoulou, J. Batita, S. Hocevar, H. K. Martalis, Catal. Today 75 (2002) 157.
- [6] G. K. Bethke, H. H. Kung, Appl. Catal. 194-195 (2000) 43.
- [7] M. J. Kahlich, H. Gasteiger, R. J. Behm, J. Catal. 182 (1999) 430.
- [8] M. M. Schubert, M. J. Kahlich, H. A. Gasteiger, R. J. Behm, J. Power Sources 84 (1999) 175.
- [9] S. H. Oh, R. M. Sinkevitch, J. Catal. 142 (1993) 254.
- [10] M. J. Kahlich, H. A. Gasteiger, R. J. Behm, J. Catal. 171, (1997) 93.
- [11] S. Özkara, A. E. Aksoylu, Appl. Catal. A 251 (2003) 75.
- [12] A. Wootsch, C. Descorme, D. Duprez, J. Catal. 225 (2004) 259.
- [13] Y.-F. Han, M. J. Kahlich, M. Kinne, R. J. Behm, Phys. Chem. Chem. Phys. 4 (2002) 389.
- [14] M. M. Schubert, M. J. Kahlich, G. Feldmeyer, M. Hüttner, S. Hackensberg, H. A. Gasteiger, R. J. Behm, Phys. Chem. Chem. Phys. 3 (2001) 1123.
- [15] F. Marino, C. Descorme, D. Duprez, Appl. Catal. B. Environ. 58 (2005) 175.
- [16] W.-J. Shen, Y. Ichihashi, H. Ando, Y. Matsumura, M. Okumura, M. Haruta, Appl. Catal. A 217 (2001) 231.
- [17] A. Martínez-Arias, A. B. Hungaria, M. Fernández-García, A. Iglesias-Juez, J. A. Anderson, J. C. Conesa, J. Catal. 221 (2004) 85.
- [18] J. A. Wang, L. F. Chen, M. A. Valenzuela, A. Montoya, J. Salamones, P. D. Angel, Appl. Surf. Sci. 230 (2004) 34.
- [19] E. Bekyarova, P. Fornasiero, J. Kaspar, M. Graziani, Catalysis Today 45 (1998) 179.
- [20] L. Gucci, A. Beck, A. Horváth, Zs. Koppány, G. Stefler, K. Frey, I. Sajó, O. Gesztí, D. Bazin, J. Lynch, J. Mol. Catal. A. 204-205 (2003) 545.
- [21] F. Marino, C. Descorme, D. Duprez, Appl. Catal. B 54 (2004) 59.
- [22] W. Li, F. J. Garcia, E. E. Wolf, Catal. Today 81 (2003) 437.
- [23] I. Rosso, C. Galletti, G. Saracco, E. Garrone, V. Specchia, Appl. Catal. B. 48 (2004) 195.
- [24] S. Bedrane, C. Descorme, D. Duprez, Catalysis Today 73 (2002) 233.
- [25] S. Bedrane, C. Descorme, D. Duprez, Catalysis Today 75 (2002) 401.
- [26] Y. Madiér, C. Descorme, A. M. Le Govic, D. Duprez, J. Phys. Chem. B. 103 (1999) 10999.
- [27] D. Teschner, A. Wootsch, K. Matusek, T. Röder, Z. Paál, Solid State Ionics, 141 (2001) 709.
- [28] S. Kacimi, J. Barbier Jr., R. Taha, D. Duprez, Catal. Lett. 22 (1993) 343.
- [29] A. Holmgren, B. Andersson, J. Catal. 178 (1998) 14.
- [30] A. Palazov, C. C. Chang, R. J. Kokes, J. Catal. 36 (1975) 338.
- [31] R. P. Eischens, S. A. Francis, W. A. Pliskin, J. Phys. Chem. 60 (1956) 194.
- [32] F. Bozon-Verduraz, A. Bensalem, J. Chem. Soc. Faraday Trans. 1 90 (1994) 653.
- [33] A. Palazov, G. Kadinov, C. Bonev, D. Shopov, J. Catal. 74 (1982) 44.
- [34] A. M. Bradshaw, F. M. Hoffmann, Surf. Sci. 72 (1978) 513.
- [35] A. Badri, C. Binet, J. C. Lavalley, J. Chem. Soc., Faraday Trans., 92 (1996) 4669.
- [36] C. Binet, A. Badri, J. C. Lavalley, J. Phys. Chem. 98 (1994) 6392.
- [37] G. Jacobs, U. M. Graham, E. Chenu, P. M. Patterson, A. Dozier, B. H. Davis, J. Catal. 229 (2005) 499.
- [38] C. Li, Y. Sakata, T. Arai, K. Domen, K. Maruya, T. Onishi, J. Chem. Soc. Faraday Trans. 85 (1989) 1451.

- [39] G. Busca, J. Lamotte, J. C. Lavalley, V. Lorinzelli, J. Am. Chem. Soc. 109 (1987) 5197.
- [40] D. Teschner, A. Pestryakov, E. Kleimenov, M. Hävecker, H. Bluhm, H. Sauer, A. Knop-Gericke, R. Schlögl, J. Catal. 230 (2005) 186.
- [41] A. Doyle, Sh. Shaikhutdinov, S. D. Jackson, H.-J. Freund, Ang. Chem. 42 (2003) 5240.
- [42] G. Rupprechter, M. Morkel, H.-J. Freund, R. Hirschl, Surf. Sci. 554 (2004) 43.
- [43] M. G. Ramsey, F. P. Leisenberger, F. P. Netzer, A. J. Roberts, R. Raval, Surf. Sci. 385 (1997) 207.
- [44] G. Comelli, M. Sastry, L. Olivi, G. Paolucci, K. C. Prince, Phys. Rev. B 43 (1991) 14385.
- [45] N. Tsud, V. Dudr, S. Fabík, C. Brun, V. Cháb, V. Matolín, K.C. Prince, Surf. Sci. 560 (2004) 259.
- [46] D. R. Mullins, S. H. Overbury, D. R. Huntley, Surf. Sci. 409 (1998) 307.
- [47] A. Q. Wang, P. Panchaipetch, R. M. Wallace, T. D. Golden, J. Vac. Sci. Technol. B 21 (2003) 1169.
- [48] E. A. Kümmerle, G. Heger, J. Sol. State Chem. 147 (1999) 485.
- [49] A. B. Mhadeswar, D. G. Vlachos, J. Phys Chem. B. 108 (2004) 15246.